A high-order doubly asymptotic open boundary for scalar waves in semi-infinite layered systems

S. Prempramote[1], C. Birk[2] and Ch. Song[1]

[1] School of Civil & Environmental Engineering, University of New South Wales, Sydney 2052, Australia
[2] Institute for Structural Analysis, Department of Civil Engineering, Dresden University of Technology, Dresden 01062, Germany

E-mail: suriyon@student.unsw.edu.au, carolin.birk@tu-dresden.de and c.song@unsw.edu.au

Abstract. Wave propagation in semi-infinite layered systems is of interest in earthquake engineering, acoustics, electromagnetism, etc. The numerical modelling of this problem is particularly challenging as evanescent waves exist below the cut-off frequency. Most of the high-order transmitting boundaries are unable to model the evanescent waves. As a result, spurious reflection occurs at late time. In this paper, a high-order doubly asymptotic open boundary is developed for scalar waves propagating in semi-infinite layered systems. It is derived from the equation of dynamic stiffness matrix obtained in the scaled boundary finite-element method in the frequency domain. A continued-fraction solution of the dynamic stiffness matrix is determined recursively by satisfying the scaled boundary finite-element equation at both high- and low-frequency limits. In the time domain, the continued-fraction solution permits the force-displacement relationship to be formulated as a system of first-order ordinary differential equations. Standard time-step schemes in structural dynamics can be directly applied to evaluate the response history. Examples of a semi-infinite homogeneous layer and a semi-infinite two-layered system are investigated herein. The displacement results obtained from the open boundary converge rapidly as the order of continued fractions increases. Accurate results are obtained at early time and late time.

1. Introduction

The problem of scalar waves propagating in a semi-infinite layered system, as shown in Fig. 1(a) occurs in the study of acoustics, composites, earthquake engineering and electromagnetism. To be able to account for nonlinearities occurring in the near field, a transmitting boundary formulated directly in the time domain has to be applied to represent the wave propagation to infinity. Various transmitting boundaries have been proposed for a semi-infinite homogeneous layer [1–3]. Recently, high-order transmitting boundaries [4–10] have been developed to improve the accuracy and efficiency of the low-order ones. A doubly asymptotic open boundary constructed in [11] is used for a semi-infinite homogeneous layer. The two-dimensional problem is decomposed into a series of one-dimensional problems by using the method of separation of variables. It is shown by examining the modal dynamic stiffness in the frequency domain that most of high-order transmitting boundaries are singly asymptotic at the high-frequency limit. Thus, they are appropriate only for radiative fields i.e. virtually all of the field energy propagates out to infinity. However, a cut-off frequency exists in a semi-infinite homogeneous layer. Below the cut-off frequency, evanescent waves present. When the excitation frequency is lower than the cut-off frequency, numerical pollution, which is similar to the fictitious reflection at a fixed or free boundary, occurs in a long time analysis [11]. The study of semi-infinite layered systems directly in the time domain is rarely reported in the literature. As a transformation to a series of one-dimensional problems by the method of separation of variables is no longer possible, many of the techniques of constructing high-order transmitting boundaries are no longer applicable.

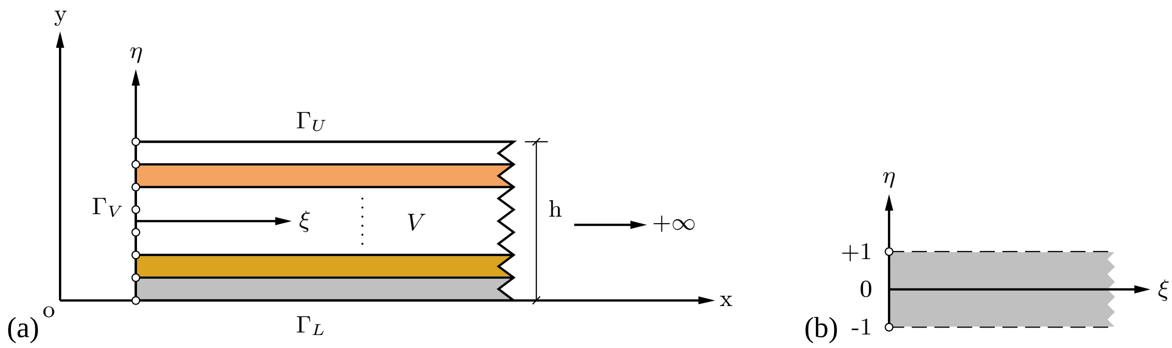

Figure 1. Semi-infinite layered system: (a) geometry and (b) scaled boundary coordinates

In this paper, a doubly asymptotic open boundary condition is developed for semi-infinite layered systems. An equation of the dynamic stiffness matrix of a layered system is obtained by using the scaled boundary finite-element method. A doubly asymptotic solution of the dynamic stiffness matrix is formulated as continued fractions. The force-displacement relationship is expressed as a system of first-order ordinary differential equations in the time domain after introducing auxiliary variables. The formulation is local in time. Thus well-established time-stepping schemes in structural dynamics are directly applicable.

2. Scaled boundary finite-element method for semi-infinite layered systems

A semi-infinite layered system with a constant depth h is shown in Fig. 1(a). The out-of-plane (anti-plane) motion $u = u(x, y, t)$ is considered. The governing differential equation of motion is written as

$$G(u_{,xx} + u_{,yy}) = \rho \ddot{u} \tag{1}$$

where G and ρ are the shear modulus and mass density of a layer. The Neumann boundary condition is imposed on the upper boundary Γ_U (i.e. $u_{,y}(y = h) = 0$), and the Dirichlet boundary condition is imposed on the lower boundary (i.e. $u(y = 0) = 0$). The conditions of equilibrium and compatibility have to be satisfied at the interface between two layers. A distributed force $f(y, t)$ is applied along the vertical boundary Γ_V located at $x = x_b$.

The scaled boundary finite-element method (SBFEM) is employed. The derivation of the scaled boundary finite-element equations in dynamic stiffness and in displacement are available in [12, 13]. Only the key concept is summarized in the following:

The vertical boundary is divided into line elements as shown in Fig. 1(a). The shape functions $[N(\eta)]$ are defined in the local coordinate η. The geometry of the element is described by

$$y_b(\eta) = [N(\eta)]\{y_b\} \tag{2}$$

where $\{y_b\}$ are the nodal coordinates. The semi-infinite layered system is obtained by continuously shifting the boundary as shown in Fig. 1(b) for one element on the boundary. The coordinate transformation is expressed as

$$x(\xi) = x_b + \xi \tag{3a}$$
$$y(\xi, \eta) = [N(\eta)]\{y_b\} \tag{3b}$$

where ξ and η are the scaled boundary coordinates.

A displacement function $\{u(\xi)\}$ is defined on a horizontal line passing through a node on the vertical boundary Γ_V. The displacements in the layers are approximated by interpolating the displacement functions piecewisely

$$\{u(\xi,\eta)\} = [N(\eta)]\{u(\xi)\} \tag{4}$$

By transforming the governing equation (Eq. (1)) to the scaled boundary coordinates (Eq. (3)) and applying the Galerkin's weighted residual method along the vertical direction, the scaled boundary finite-element equation in displacement is formulated as

$$[E^0]\{u(\xi)\}_{,\xi\xi} - [E^2]\{u(\xi)\} - [M^0]\{\ddot{u}(\xi)\} = 0 \tag{5}$$

where $[E^0]$, $[E^2]$ and $[M^0]$ are the coefficient matrices obtained from the assembling of the element coefficient matrices as in the finite element method [12]. In the frequency domain (excitation frequency ω), Eq. (5) is expressed as

$$[E^0]\{U(\xi)\}_{,\xi\xi} - [E^2]\{U(\xi)\} + \omega^2[M^0]\{U(\xi)\} = 0 \tag{6}$$

with the amplitude of the displacement functions $\{U(\xi)\}$. The amplitude of the internal nodal forces along the horizontal lines are obtained from the integration of the surface traction over the elements

$$\{Q(\xi)\} = [E^0]\{U(\xi)\}_{,\xi} \tag{7}$$

Since the outward normal of the vertical boundary Γ_V is opposite to the x-direction, the dynamic stiffness matrix $[S^\infty(\omega)]$ relating the amplitude of the force and displacement functions is defined in

$$-\{Q(\xi)\} = [S^\infty(\omega)]\{U(\xi)\} \tag{8}$$

By eliminating the terms $\{Q(\xi)\}$ and $\{U(\xi)\}$ in Eqs. (6), (7) and (8), the scaled boundary finite-element equation in dynamic stiffness is expressed as

$$[S^\infty(\omega)][E^0]^{-1}[S^\infty(\omega)] - [E^2] + \omega^2[M^0] = 0 \tag{9}$$

Equation (9) is simplified by using the following general eigenvalue problems of $[E^0]$ and $[M^0]$ ($\lceil\cdot\rfloor$ stands for a diagonal matrix)

$$[M^0][\Phi] = [E^0][\Phi]\lceil\Lambda^2\rfloor/c_s^2 \tag{10a}$$
$$[\Phi]^T[E^0][\Phi] = [I] \tag{10b}$$

The eigenvalues $\lceil\Lambda^2\rfloor/c_s^2$ and eigenvectors $[\Phi]$ obtained from the eigen-decomposition in Eq. (10a) can satisfy the orthogonality condition in Eq. (10b). The shear wave speed $c_s = \sqrt{G/\rho}$ is chosen as that of the softest layer. By using Eq. (10), Eq. (9) is transformed to

$$[\widetilde{S}(a_0)]^2 + a_0^2\lceil\Lambda^2\rfloor - [\widetilde{E}^2] = 0 \tag{11}$$

with

$$[\widetilde{S}(a_0)] = h[\Phi]^T[S^\infty(\omega)][\Phi] \tag{12a}$$
$$[\widetilde{E}^2] = h^2[\Phi]^T[E^2][\Phi] \tag{12b}$$

and the dimensionless frequency

$$a_0 = \frac{\omega h}{c_s} \tag{13}$$

At a specified frequency, the solution for the transformed dynamic stiffness matrix $[\widetilde{S}(a_0)]$ can be obtained from Eq. (11) directly by solving the eigenvalue problem

$$([\widetilde{E}^2] - a_0^2\lceil\Lambda^2\rfloor)[\Psi] = [\Psi]\lceil\Omega^2\rfloor \tag{14}$$

where the entries of $\lceil\Omega\rfloor$ are either positive real numbers or purely positive imaginary numbers. The solution for the transformed dynamic stiffness matrix is expressed as

$$[\widetilde{S}(a_0)] \quad = \quad [\Psi]\lceil\Omega\rfloor[\Psi]^{-1} \tag{15}$$

3. Doubly asymptotic continued-fraction solution for transformed dynamic stiffness matrix

To obtain the doubly asymptotic continued-fraction solution, the continued-fraction solution at the high-frequency limit is addressed first

$$[\widetilde{S}(a_0)] \quad = \quad [\widetilde{K}] + \mathrm{i}a_0[\widetilde{C}] - [\widetilde{Y}^{(1)}(a_0)]^{-1} \tag{16}$$

where $[\widetilde{K}]$ and $[\widetilde{C}]$ are coefficient matrices and $[\widetilde{Y}^{(1)}(a_0)]$ a residual term. Substituting Eq. (16) into Eq. (11) and setting the coefficients of the power series of $\mathrm{i}a_0$ to zero lead to the solutions

$$[\widetilde{C}] = \lceil\Lambda\rfloor; \quad [\widetilde{K}] = 0 \tag{17}$$

and an equation of $[\widetilde{Y}^{(1)}(a_0)]$ expressed as the $i = 1$ case of

$$[\widetilde{Y}^{(i)}(a_0)][\tilde{c}^{(i)}][\widetilde{Y}^{(i)}(a_0)] - \mathrm{i}a_0[\tilde{b}_1^{(i)}][\widetilde{Y}^{(i)}(a_0)] - \mathrm{i}a_0[\widetilde{Y}^{(i)}(a_0)][\tilde{b}_1^{(i)}]^T + [\tilde{a}^{(i)}] \quad = \quad 0 \tag{18}$$

with

$$[\tilde{a}^{(1)}] \quad = \quad [I] \tag{19a}$$
$$[\widetilde{V}^{(1)}] \quad = \quad [I] \tag{19b}$$
$$[\tilde{b}_1^{(1)}] \quad = \quad [\widetilde{C}] = [\widetilde{V}^{(1)}]\lceil\Lambda\rfloor[\widetilde{V}^{(1)}]^{-1} \tag{19c}$$
$$[\tilde{c}^{(1)}] \quad = \quad -[\widetilde{E}^2] \tag{19d}$$

The residual term $[\widetilde{Y}^{(i)}(a_0)]$ is decomposed as

$$[\widetilde{Y}^{(i)}(a_0)] \quad = \quad \mathrm{i}a_0[\widetilde{Y}_1^{(i)}] - [\widetilde{Y}^{(i+1)}(a_0)]^{-1} \qquad (i = 1, 2, 3, ..., M_H) \tag{20}$$

where $[\widetilde{Y}_1^{(i)}]$ is a coefficient matrix. The constant term is not included as its solution vanishes. By substituting Eq. (20) into Eq. (18), the solution for $[\widetilde{Y}_1^{(i)}]$ is obtained from

$$[\widetilde{Y}_1^{(i)}]^{-1} \quad = \quad [\widetilde{V}^{(i)}]^{-T}[\tilde{y}_1^{(i)}]^{-1}[\widetilde{V}^{(i)}]^{-1} \tag{21}$$

where $[\tilde{y}_1^{(i)}]^{-1}$ is the solution for

$$\lceil\Lambda\rfloor[\tilde{y}_1^{(i)}]^{-1} + [\tilde{y}_1^{(i)}]^{-1}\lceil\Lambda\rfloor - [\widetilde{V}^{(i)}]^T[\tilde{c}^{(i)}][\widetilde{V}^{(i)}] \quad = \quad 0 \tag{22}$$

The equation for the residual term $[\widetilde{Y}^{(i+1)}(a_0)]$ is expressed as

$$\begin{aligned}[\widetilde{Y}^{(i+1)}(a_0)][\tilde{c}^{(i+1)}][\widetilde{Y}^{(i+1)}(a_0)] - \mathrm{i}a_0[\tilde{b}_1^{(i+1)}][\widetilde{Y}^{(i+1)}(a_0)]& \\ -\mathrm{i}a_0[\widetilde{Y}^{(i+1)}(a_0)][\tilde{b}_1^{(i+1)}]^T + [\tilde{a}^{(i+1)}] \quad &= \quad 0\end{aligned} \tag{23}$$

where the following matrices used in the recursive procedure at the high-frequency expansion are updated by

$$[\tilde{a}^{(i+1)}] = [\tilde{c}^{(i)}] \tag{24a}$$
$$[\widetilde{V}^{(i+1)}] = [\widetilde{Y}_1^{(i)}]^{-1}[\widetilde{V}^{(i)}] \tag{24b}$$
$$[\tilde{b}_1^{(i+1)}] = -[\tilde{b}_1^{(i)}]^T + [\tilde{c}^{(i)}][\widetilde{Y}_1^{(i)}] = [\widetilde{V}^{(i+1)}]\lceil\Lambda\rfloor[\widetilde{V}^{(i+1)}]^{-1} \tag{24c}$$
$$[\tilde{c}^{(i+1)}] = [\tilde{a}^{(i)}] \tag{24d}$$

In order to extend the derivation of the continued-fraction solution to the low-frequency limit, the residual term $[\widetilde{Y}^{(M_H+1)}(a_0)]$ is rewritten as $[\widetilde{Y}_L(a_0)]$ and decomposed as

$$[\widetilde{Y}^{(M_H+1)}(a_0)] = [\widetilde{Y}_L(a_0)] = [\widetilde{Y}_{L0}^{(0)}] + \mathrm{i}a_0[\widetilde{Y}_{L1}^{(0)}] - (\mathrm{i}a_0)^2[\widetilde{Y}_L^{(1)}(a_0)]^{-1} \tag{25}$$

By using Eqs. (16), (20) and (25), the dynamic stiffness matrix is expanded as

$$\begin{aligned}[\widetilde{S}(a_0)] = {} & \mathrm{i}a_0[\widetilde{C}] - (\mathrm{i}a_0[\widetilde{Y}_1^{(1)}] - (\mathrm{i}a_0[\widetilde{Y}_1^{(2)}] - \dots \\ & -(\mathrm{i}a_0[\widetilde{Y}_1^{(M_H)}] - ([\widetilde{Y}_{L0}^{(0)}] + \mathrm{i}a_0[\widetilde{Y}_{L1}^{(0)}] - (\mathrm{i}a_0)^2[\widetilde{Y}_L^{(1)}(a_0)]^{-1})^{-1})^{-1}\dots)^{-1})^{-1}\end{aligned} \tag{26}$$

and by formulating Eq. (26) with $a_0 = 0$, the coefficient matrix $[\widetilde{Y}_{L0}^{(0)}]$ is obtained as

$$[\widetilde{Y}_{L0}^{(0)}] = \begin{cases} [\widetilde{S}(a_0=0)] & \text{when } M_H \text{ is odd number} \\ -[\widetilde{S}(a_0=0)]^{-1} & \text{when } M_H \text{ is even number}\end{cases} \tag{27}$$

where the static stiffness $[\widetilde{S}(a_0 = 0)]$ is obtained from Eqs. (15) and (14). The solution for $[\widetilde{Y}_{L1}^{(0)}]$ is determined from Eq. (28) obtained by substituting Eq. (25) into Eq. (23)

$$([\widetilde{Y}_{L0}^{(0)}][\tilde{c}_L])[\widetilde{Y}_{L1}^{(0)}] + [\widetilde{Y}_{L1}^{(0)}]([\tilde{c}_L][\widetilde{Y}_{L0}^{(0)}]) - [\tilde{b}_{L1}][\widetilde{Y}_{L0}^{(0)}] - [\widetilde{Y}_{L0}^{(0)}][\tilde{b}_{L1}]^T = 0 \tag{28}$$

The residual term $[\widetilde{Y}_L^{(i)}(a_0)]$ satisfies the following equation ($i = 1$)

$$\begin{aligned}&[\widetilde{Y}_L^{(i)}(a_0)][\tilde{c}_L^{(i)}][\widetilde{Y}_L^{(i)}(a_0)] - [\widetilde{Y}_L^{(i)}(a_0)]\left([\tilde{b}_{L0}^{(i)}]^T + \mathrm{i}a_0[\tilde{b}_{L1}^{(i)}]^T\right) \\ &\quad - \left([\tilde{b}_{L0}^{(i)}] + \mathrm{i}a_0[\tilde{b}_{L1}^{(i)}]\right)[\widetilde{Y}_L^{(i)}(a_0)] + (\mathrm{i}a_0)^2[\tilde{a}_L^{(i)}] = 0\end{aligned} \tag{29}$$

with the coefficient matrices

$$[\tilde{a}_L^{(1)}] = [\tilde{c}_L] \tag{30a}$$
$$[\tilde{b}_{L0}^{(1)}] = [\tilde{c}_L][\widetilde{Y}_{L0}^{(0)}] \tag{30b}$$
$$[\tilde{b}_{L1}^{(1)}] = -[\tilde{b}_{L1}]^T + [\tilde{c}_L][\widetilde{Y}_{L1}^{(0)}] \tag{30c}$$
$$[\tilde{c}_L^{(1)}] = -[\tilde{b}_{L1}][\widetilde{Y}_{L1}^{(0)}] - [\widetilde{Y}_{L1}^{(0)}][\tilde{b}_{L1}]^T + [\widetilde{Y}_{L1}^{(0)}][\tilde{c}_L][\widetilde{Y}_{L1}^{(0)}] \tag{30d}$$

The residual term $[\widetilde{Y}_L^{(i)}(a_0)]$ is decomposed as

$$[\widetilde{Y}_L^{(i)}(a_0)] = [\widetilde{Y}_{L0}^{(i)}] + \mathrm{i}a_0[\widetilde{Y}_{L1}^{(i)}] - (\mathrm{i}a_0)^2[\widetilde{Y}_L^{(i+1)}(a_0)]^{-1} \qquad (i = 1, 2, 3, ..., M_L) \tag{31}$$

with the coefficient matrices $[\widetilde{Y}_{L0}^{(i)}]$ and $[\widetilde{Y}_{L1}^{(i)}]$. By substituting Eq. (31) into Eq. (29), the solution for $[\widetilde{Y}_{L0}^{(i)}]$ is determined from

$$[\widetilde{Y}_{L0}^{(i)}]^{-1} = [\widetilde{V}_L^{(i)}]^{-T}[\tilde{y}_{L0}^{(i)}]^{-1}[\widetilde{V}_L^{(i)}]^{-1} \tag{32}$$

where $[\tilde{y}_{L0}^{(i)}]^{-1}$ is the solution for

$$\lceil \Lambda_L \rfloor [\tilde{y}_{L0}^{(i)}]^{-1} + [\tilde{y}_{L0}^{(i)}]^{-1} \lceil \Lambda_L \rfloor - [\widetilde{V}_L^{(i)}]^T [\tilde{c}_L^{(i)}][\widetilde{V}_L^{(i)}] \quad = \quad 0 \tag{33}$$

The eigenvalues $\lceil \Lambda_L \rfloor$ are obtained from the eigen-decomposition

$$[\tilde{b}_{L0}^{(i)}] \quad = \quad [\widetilde{V}_L^{(i)}] \lceil \Lambda_L \rfloor [\widetilde{V}_L^{(i)}]^{-1} \tag{34}$$

where $[\widetilde{V}_L^{(i)}]$ are the eigenvectors. The solution for $[\widetilde{Y}_{L1}^{(i)}]$ is determined from

$$[\widetilde{Y}_{L1}^{(i)}] \quad = \quad [\widetilde{V}_L^{(i+1)}]^{-T} [\tilde{y}_{L1}^{(i)}][\widetilde{V}_L^{(i+1)}]^{-1} \tag{35}$$

where $[\widetilde{V}_L^{(i+1)}]$ is defined as

$$[\widetilde{V}_L^{(i+1)}] \quad = \quad [\widetilde{Y}_{L0}^{(i)}]^{-1} [\widetilde{V}_L^{(i)}] \tag{36}$$

and $[\tilde{y}_{L1}^{(i)}]$ is the solution for

$$\lceil \Lambda_L \rfloor [\tilde{y}_{L1}^{(i)}] + [\tilde{y}_{L1}^{(i)}] \lceil \Lambda_L \rfloor - [\widetilde{V}_L^{(i+1)}]^T [\tilde{b}_{L1}^{(i)}][\widetilde{V}_L^{(i)}] - [\widetilde{V}_L^{(i)}]^T [\tilde{b}_{L1}^{(i)}]^T [\widetilde{V}_L^{(i+1)}] \quad = \quad 0 \tag{37}$$

The following matrices used in the recursive procedure at the low-frequency expansion are updated by

$$[\tilde{a}_L^{(i+1)}] \quad = \quad [\tilde{c}_L^{(i)}] \tag{38a}$$
$$[\tilde{b}_{L0}^{(i+1)}] \quad = \quad -[\tilde{b}_{L0}^{(i)}]^T + [\tilde{c}_L^{(i)}][\widetilde{Y}_{L0}^{(i)}] = [\widetilde{V}_L^{(i+1)}] \lceil \Lambda_L \rfloor [\widetilde{V}_L^{(i+1)}]^{-1} \tag{38b}$$
$$[\tilde{b}_{L1}^{(i+1)}] \quad = \quad -[\tilde{b}_{L1}^{(i)}]^T + [\tilde{c}_L^{(i)}][\widetilde{Y}_{L1}^{(i)}] \tag{38c}$$
$$[\tilde{c}_L^{(i+1)}] \quad = \quad [\tilde{a}_L^{(i)}] - [\tilde{b}_{L1}^{(i)}][\widetilde{Y}_{L1}^{(i)}] - [\widetilde{Y}_{L1}^{(i)}][\tilde{b}_{L1}^{(i)}]^T + [\widetilde{Y}_{L1}^{(i)}][\tilde{c}_L^{(i)}][\widetilde{Y}_{L1}^{(i)}] \tag{38d}$$

4. High-order doubly asymptotic open boundary

By using the doubly asymptotic solution of the dynamic stiffness matrix of the layered system, the force $\{R\}$-displacement $\{U\} = \{U(\xi = 1)\}$ relationship on the vertical boundary Γ_V

$$\{R\} = [S^\infty(\omega)]\{U\} \tag{39}$$

can be formulated as an open boundary by introducing the auxiliary variables. The formulation is expressed in the frequency domain as

$$([K_h] + \mathrm{i}\omega[C_h])\{Z\} \quad = \quad \{F\} \tag{40}$$

with

$$\{Z\} \quad = \quad [\{U\}, \{\widetilde{U}^{(1)}\}, ..., \{\widetilde{U}^{(M_H)}\}, \{\widetilde{U}_L^{(0)}\}, \{\widetilde{U}_L^{(1)}\}, ..., \{\widetilde{U}_L^{(M_L)}\}]^T \tag{41a}$$
$$\{F\} \quad = \quad [\{R\}, 0, ..., 0, 0, 0, ...,0]^T \tag{41b}$$

$\{\widetilde{U}^{(i)}\}$ $(i = 1, 2, \ldots, M_H)$ and $\{\widetilde{U}_L^{(i)}\}$ $(i = 0, 1, \ldots, M_L)$ are the auxiliary variables. The static stiffness matrix $[K_h]$ and the damping matrix $[C_h]$ are symmetric

$$[K_h] \quad = \quad \frac{1}{h} \begin{bmatrix} 0 & -[\Phi]^{-T} & & & & & & \\ -[\Phi]^{-1} & 0 & -[I] & & & & & \\ & -[I] & \ddots & \ddots & & & & \\ & & \ddots & 0 & -[I] & & & \\ & & & -[I] & [\widetilde{Y}_{L0}^{(0)}] & 0 & & \\ & & & & 0 & [\widetilde{Y}_{L0}^{(1)}] & \ddots & \\ & & & & & \ddots & \ddots & 0 \\ & & & & & & 0 & [\widetilde{Y}_{L0}^{(M_L)}] \end{bmatrix} \tag{42a}$$

$$[C_h] = \frac{1}{c_s}\left[\begin{array}{ccccccccc} [\Phi]^{-T}[\widetilde{C}][\Phi]^{-1} & 0 & & & & & & & \\ 0 & [\widetilde{Y}_1^{(1)}] & 0 & & & & & & \\ & 0 & \ddots & \ddots & & & & & \\ & & \ddots & [\widetilde{Y}_1^{(M_H)}] & 0 & & & & \\ & & & 0 & [\widetilde{Y}_{L1}^{(0)}] & -[I] & & & \\ & & & & -[I] & [\widetilde{Y}_{L1}^{(1)}] & \ddots & & \\ & & & & & \ddots & \ddots & -[I] & \\ & & & & & & -[I] & [\widetilde{Y}_{L1}^{(M_L)}] & \end{array}\right] \tag{42b}$$

Equation (40) is written in the time domain as a system of first-order ordinary differential equations

$$[K_h]\{z(t)\} + [C_h]\{\dot{z}(t)\} = \{f(t)\} \tag{43}$$

This equation represents a high-order doubly asymptotic open boundary that is local in time.

As shown in [11], most of existing high-order transmitting boundaries are singly asymptotic. Such high-order singly asymptotic transmitting boundaries can be constructed by neglecting the terms of the low-frequency expansion.

5. Numerical examples

5.1. Semi-infinite homogeneous layer

A semi-infinite homogeneous layer with depth h is shown in Fig. 2(a). The material constants are shear modulus G and mass density ρ. The shear wave speed is $c_s = \sqrt{G/\rho}$. The dimensionless frequency is defined as $a_0 = \omega h/c_s$ and the dimensionless time as $\bar{t} = tc_s/h$. The scaled boundary finite-element mesh of 12 two-node elements is shown in Fig. 2(b). The mesh is fine enough to represent waves with a dimensionless frequency up to $a_0 = 6$.

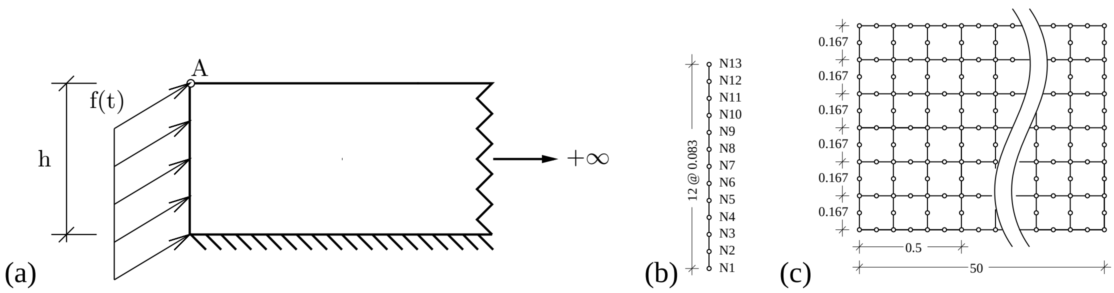

Figure 2. Semi-infinite homogeneous layer: (a) geometry, (b) SBFE mesh and (c) FE mesh

In the frequency-domain analysis, an equivalent dynamic-stiffness coefficient $S(a_0) = \{\phi\}^T[S^\infty(a_0)]\{\phi\}$ is determined by enforcing a displacement pattern $\{\phi\}$ which varies linearly from 0 to 1 along the vertical boundary Γ_V [12]. The real and imaginary parts of $S(a_0)$ non-dimensionalized by G are plotted in Fig. 3 for the doubly asymptotic continued fraction solution with $M_H = M_L = 3$ and the singly asymptotic continued fraction solution with $M_H = 7$. The result obtained from directly computing the scaled boundary finite-element solution in the frequency domain using Eqs. (15) and (14) is shown as the reference solution.

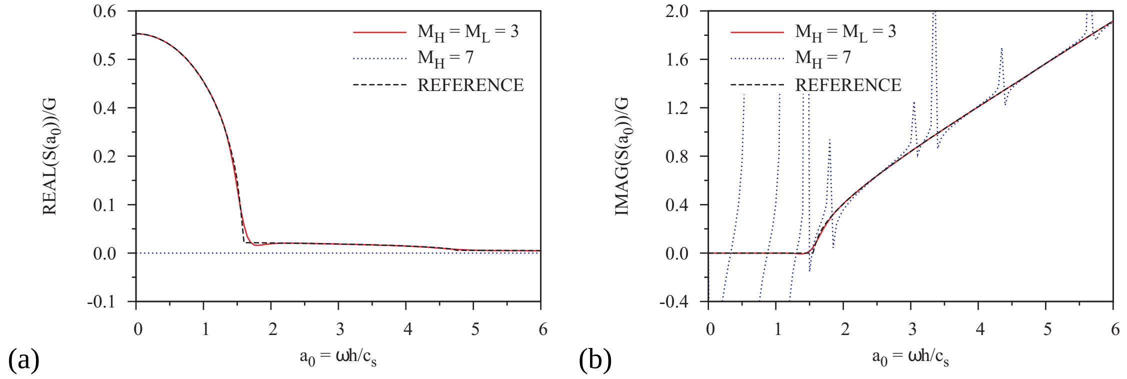

Figure 3. Doubly asymptotic continued fraction solution for equivalent dynamic-stiffness coefficient of homogeneous layer: (a) real part and (b) imaginary part

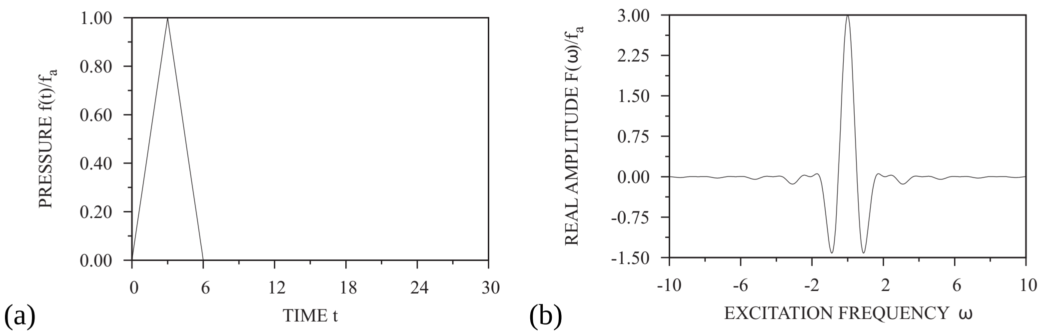

Figure 4. Force history: (a) time domain and (b) frequency domain

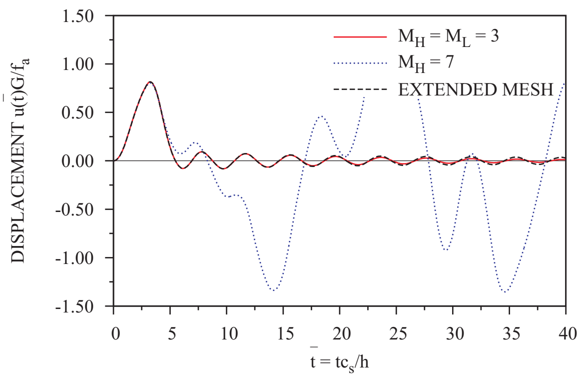

Figure 5. Displacement responses at Point A of homogeneous layer

The transient response of the homogeneous layer subjected to a uniformly distributed pressure $f(t)$ on the vertical boundary Γ_V is analyzed. The time dependence and the frequency contents are plotted in Fig. 4. The maximum value of the triangular impulse is denoted as f_a. The highest frequency of interest is $a_h = 6$. Newmark's method with $\gamma = 0.5$ and $\beta = 0.25$ (average acceleration scheme) is adopted for the time integration. The shortest dimensionless wave period $\overline{T} = 2\pi/a_h$ of interest is 1.05. The time step $\Delta\bar{t}$ is chosen as 0.05. The displacement response at Point A located at the top of the vertical boundary Γ_V (Fig. 2(a)) is plotted in Fig. 5. The result of the doubly asymptotic open boundary agrees well with that of the extended mesh of finite elements in Fig. 2(c). The result of the singly asymptotic boundary at early time ($\bar{t} = 4$) is accurate, but strong "fictitious reflection" occurs at late time.

5.2. Semi-infinite two-layered system

A two-layered system with depth $h_1 = h_2 = h/2$ is shown in Fig. 6(a). The shear modulus and mass density are G_1 and ρ_1, respectively, for Layer 1, and $G_2 = 9G_1$ and $\rho_2 = \rho_1$ for Layer 2. The ratio of the shear wave speed in Layer 2 c_{s2} to that in Layer 1 c_{s1} is equal to 3. The dimensionless frequency and time are defined as $a_0 = \omega h/c_{s1}$ and $\bar{t} = tc_{s1}/h$, respectively. The scaled boundary finite-element mesh is shown in Fig. 6(b).

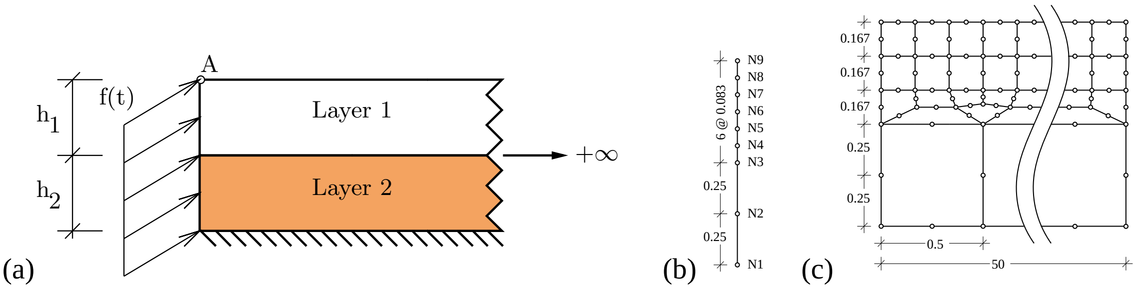

Figure 6. Semi-infinite two-layered system: (a) geometry, (b) SBFE mesh and (c) FE mesh

The equivalent dynamic-stiffness coefficient obtained from the doubly asymptotic open boundary with $M_H = M_L = 4$ is plotted in Fig. 7. It agrees well with the reference solution obtained from Eqs. (15) and (14). On the other hand, the result of the singly asymptotic continued fraction solution shows significant difference from the reference solution.

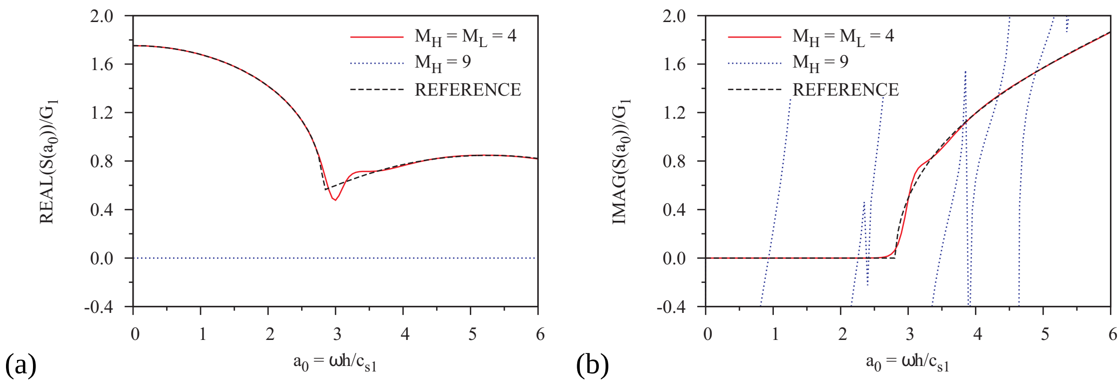

Figure 7. Doubly asymptotic continued fraction solution for equivalent dynamic-stiffness coefficient of two-layered system: (a) real part and (b) imaginary part

The response of the layered system subjected to the pressure $f(t)$ in Fig. 4(a) is analyzed. The displacement at Point A located at the top of the vertical boundary in Fig. 6(a) is plotted in Fig. 8 as a function of the dimensionless time $\bar{t}$. The result obtained from the extended mesh in Fig. 6(c) is shown as the reference solution. It can be seen that an accurate result is obtained from the doubly asymptotic open boundary. Again, significant "fictitious reflection" is observed from the singly asymptotic boundary.

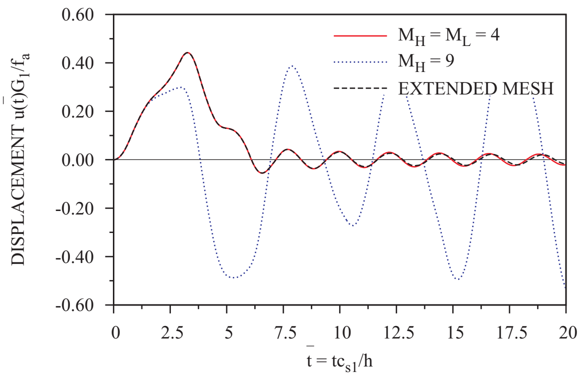

Figure 8. Displacement responses at Point A of two-layered system

6. Conclusion

The high-order doubly asymptotic open boundary has been constructed herein for the modelling of scalar wave propagation in semi-infinite layered systems. The results of a homogeneous layer and a two-layered system are presented. It can be concluded that

(i) In the frequency domain, the singly asymptotic continued fraction solution alone cannot model evanescent waves below the cut-off frequencies. This deficiency is overcome by the doubly asymptotic continued fraction solution.

(ii) In the time domain, the doubly asymptotic open boundary is accurate throughout the whole duration, while the singly asymptotic boundary is accurate only at early time.

(iii) The high-order doubly asymptotic open boundary is expressed as a system of first-order ordinary differential equations in time with constant static stiffness matrix $[K_h]$ and damping matrix $[C_h]$ that are symmetric. It can be coupled seamlessly with finite elements.

References

[1] Z. P. Liao and H. L. Wong. A transmitting boundary for the numerical simulation of elastic wave propagation. *Soil Dynamics and Earthquake Engineering*, 3:174–183, 1984.

[2] A. Bayliss, M. Gunzburger, and E. Turkel. Boundary conditions for the numerical solution of elliptic equations in exterior regions. *SIAM Journal on Applied Mathematics*, 42:430–451, 1982.

[3] Robert L. Higdon. Absorbing boundary conditions for difference approximations to the multi-dimensional wave equation. *Mathematics of Computation*, 47(176):437–459, 1986.

[4] T Hagstrom and S. I. Hariharan. A formulation of asymptotic and exact boundary conditions using local operators. *Applied Numerical Mathematics*, 27:403–416, 1998.

[5] M. J. Grote and J. B. Keller. Exact nonreflecting boundary condition for elastic waves. *SIAM Journal of Applied Mathematics*, 60:803–819, 2000.

[6] M. N. Guddati and J. L. Tassoulas. Continued-fraction absorbing boundary conditions for the wave equation. *Journal of Computational Acoustics*, 8:139–156, 2000.

[7] L. L. Thompson, R. N. Huan, and D. T. He. Accurate radiation boundary conditions for the two-dimensional wave equationon unbounded domains. *Computer Methods in Applied Mechanics and Engineering*, 191:311–351, 2001.

[8] S. Krenk. Unified formulation of radiation conditions for the wave equation. *International Journal for Numerical Methods in Engineering*, 53:275–295, 2002.

[9] D. Givoli and B. Neta. High-order non-reflecting boundary scheme for time-dependent waves. *Journal of Computational Physics*, 186:24–46, 2003.

[10] T. Hagstrom and T. Warburton. A new auxiliary variable formulation of high-order local radiation boundary conditions: Corner compatibility conditions and extensions to first-order systems. *Wave Motion*, 39:327–338, 2004.

[11] S. Prempramote, Ch. Song, F. Tin-Loi, and G. Lin. High-order doubly asymptotic open boundaries for scalar wave equation. *International Journal for Numerical Methods in Engineering*, 79:340–374, 2009.

[12] J. P. Wolf and Ch. Song. *Finite-Element Modelling of Unbounded Media*. John Wiley & Sons, Chichester, 1996.

[13] B. Li, L. Cheng, and A. J. Deeks. A modified scaled boundary finite-element method for problems with parallel side-faces. part I. theoretical developments. *Applied Ocean Research*, 27:216–223, 2005.